QuEST
BORN TO ENGINEER

numerical analysis of curved composite using cohesive zone modelling

This paper presents the finite element (FE) analysis of top hat stiffeners (manufactured using vacuum assisted resin transfer moulding (VARTM)) under static load where laminate splitting/delamination is the primary mode of failure.

Dr. Raju
QuEST Global

contents

© 2015, QuEST Global Services

Abstract

This paper presents the finite element (FE) analysis of top hat stiffeners (manufactured using vacuum assisted resin transfer moulding (VARTM)) under static load where laminate splitting/delamination is the primary mode of failure. A set of experiments are conducted on composite top hat stiffeners with three different layup arrangements. The experimental study together with FE modelling to capture the delamination failure is presented. Fracture initiation is predicted using an inter-laminar strength-based criterion. A fracture mechanics - based formulation is used to predict the delamination propagation by connecting the composite layers with 2D/3D interface elements. A reasonable agreement between the experiment and finite element analysis has been observed. Factors affecting the fibre-matrix interface strength were studied. The failure location and failure mode for fracture initiation and propagation are determined.

Keywords: curved composites; delamination; progressive failure analysis; cohesive zone element;

Introduction

The failure modes in composites include matrix cracking, fibre breakage, delamination and interface (tibre/malrix) debonding. In structural composites, the initiation of a crack/fracture does not indicate ultimate failure. Generally, a stable crack propagation stage, associated with steady increase in external load, precedes a catastrophic failure. This is frequently observed in structural applications of composites. In this paper, analytical and experimental investigation of composite top hat stiffeners is studied. Design and assessment of such structures require adequate consideration of strength and fracture toughness.

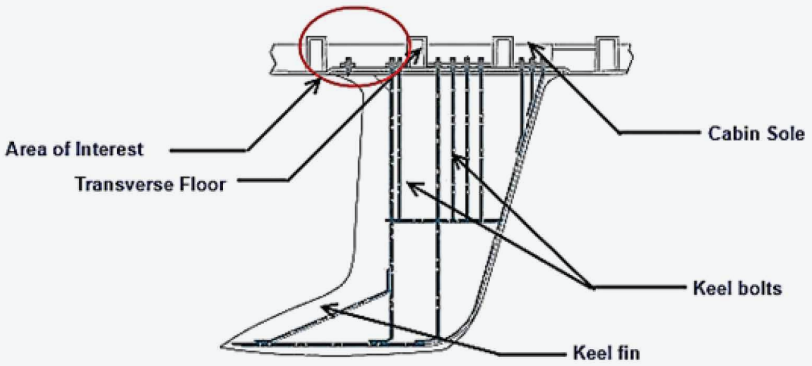

Fig. 1. Keel-hull assembly

The keel on a sailing yacht is normally attached using a series of bolts which penetrate the hull. These bolts load the hull through washer plates, which bear down upon the flanges of top-hat stiffeners called keel floors .With such high loadings (combination of tensile / compression, flexure and torsional loads), the design of supporting structure in this region is critical. However, because of complex loading, this region is often over-designed to prevent failure. Thus it is necessary to focus on the structural design of keel structure to minimise human and material losses, which can be achieved by understanding the interlaminar tensile and shear stress distribution and their effect on composite failures. This determines the load-carrying capacity and damage mechanism of top-hat stiffeners.

Keel bolts usually connect the keel directly to the hull laminate in pockets between transverse floors and longitudinals, relying on high compressive strength of the laminate. The structural configuration of a keel attached to a yacht hull and top-hat-stiffener (THS) is shown in Fig 1. Stainless steel bolts are normally used to attach the keel to the hull.

© 2015, QuEST Global Services

Background Study

Curved composites are inevitable in the design of many structural applications. The primary mode of failure in curved composites is delamination, which occurs when the bends are opened or closed due to external load or pressure. The stress distribution is complex in nature and delamination is caused by through-thickness tension and a lack of through-thickness strength. Delaminations are generally embedded between the composite layers and frequently go undetected. Interlaminar tensile and shear strength are the key parameters in defining delamination strength of the composite. But these two are matrix related properties and it is very difficult to increase delamination strength of the structure without external fastenings. Study of the interlaminar stress distribution at the bend helps in predicting delamination failures in curved structures. Most common sources of delaminations are generally material and structural discontinuities which are shown in Fig. 2 (Sridharan, 2008). Prevention of delamination may be possible with techniques such as fabric stitching, z-pinning, (Mouritz et al, 1997a; Mouritz et al, 1997b), but practically they may not be used due to constraints such as cost, weight, manufacturing process and complexity of analysis.

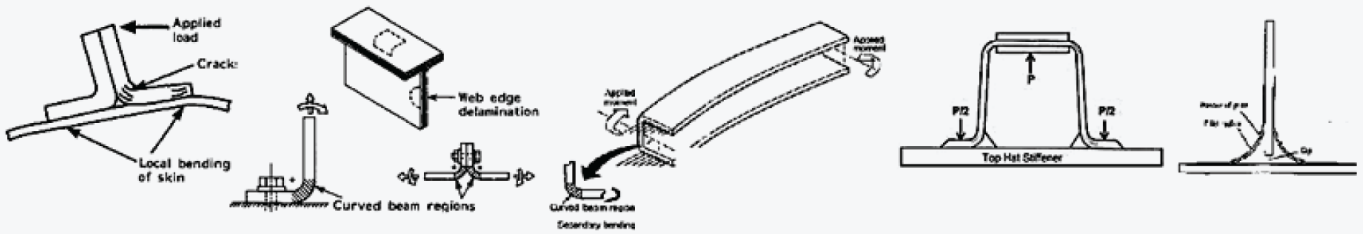

Fig. 2. Curved structures subjected to opening moments inducing interlaminar tensile stress (Kedward et al., 1989)

The stresses acting at the interface of two adjacent plies in composite laminates are called interlaminar stresses and are primarily responsible for delamination failure (Sridharan, 2008). There are three such stresses, which are interlaminar normal stress σz and interlaminar shear stresses τxz and τyz. Kedward et al. (1989) studied the radial stress distribution for a curved beam using NASTRAN 2D and 3D elements and also analytically using simplified strength of materials approach and classical elastic theory. FE codes were developed (Graff, 1989) to numerically obtain stresses and strains in curved composite strap laminates (Graphite-Epoxy, Kevlar-Epoxy, Glass-Epoxy) using the Tsai-Wu failure criterion. Comparisons between fracture mechanics and strength based delamination predictions were also made (Martin & Jackson, 1993). The problem of interlaminar tensile/compressive or shear stresses was highlighted at the bonded joints and attachments of marine composite structures (Dodkins et al. 1994). Wisnom (1996 and 1998) was one of the primary investigators to study delamination failure through experimental, analytical and numerical approaches to detect interlaminar failure and flexural strength of composite laminates. Lekhnitskii's equations (1968) are applicable only for pure bending or edge loading, thus they cannot sustain the circumferential force without radial restraints. Shenoi & Wang (2001) developed equations based on elasticity theory for delamination and flexural strength of curved composites. The effects of key variables such as stacking sequence, radius of curvature and skin thickness on stress distribution within a curved layered beam and sandwich beam were also studied. A progressive failure methodology for the laminated stiffened and unstiffened panels was presented using an arbitrarily oriented stiffener formulation (Prusty & Ray, 2005). The formulation was based on the linear, arbitrarily oriented stiffener formulation of Prusty (2003) for the analysis of laminated hat stiffened plates and shells.

© 2015, QuEST Global Services

Discussion of FEA Approaches

FEA of top-hat stiffeners

Top hat stiffeners are generally used in the fabrication of stiffened panels such as decks, bulkheads or hull shells. One other important use of top hat stiffeners is to reinforce the joining of the keel to the yacht's hull (Dodkins et al., 1994). Key benefits of top hat stiffenersand beamsare to attain high bending stiffness and torsional resistance. The prime characteristic of out-of-plane joints using layered composites is that, because of a lack of continuity of reinforcing fibres across the joint, they are susceptible to failure by peel or delamination well before the ultimate in-plane laminate material stress is reached (Dodkins et al. 1994; Raju et al. 2010). Shenoi & Hawkins (1995) numerically investigated the design of top hat stiffener to shell plating joints for ships and boats using the commercially available FE software ANSYS. The authors presented a parametric study on laminate thickness, gap size, back fill angle and fillet radius of top hat stiffener. Junhou & Shenoi (1996) proposed three loading configurations (3 point bend, reverse 3 point bend & pull off) to analyse the different failure modes of top hat stiffeners. Phillips et al. (1999) experimentally and numerically conducted these three tests and studied stress distribution at the bend of the laminate using ANSYS. Eksik et al. (2004) studied the failure of hat-shaped composite sandwich beams using a four-point bend test. Experimental and numerical study of top hat stiffened panels by Eksik et al. (2007) described critical locations of structural damage and failure mechanisms under in-service loading conditions. The current study focuses on the numerical simulation of a top hat stiffener. The distinction between stiffeners and beams is that the stiffeners are subjected primarily to axial compression and reinforce the panel against buckling whereas the beams are subjected to more general loading including transverse loads.

Delamination characterisation by FEA

During the fracture process of a curved composite, matrix bending cracks often initiate in Mode I, and are governed by transverse tensile/normal stresses. The matrix shear cracks may be governed by interlaminar shear and transverse tensile stresses (Choi et al. 1991). There are two different techniques to simulate the delamination mechanism. The first approach is based on strength criteria and the second is based on fracture mechanics criteria. The strength based formulation assumes the material to be free of defects and generally uses interlaminar failure criteria. The stress in the material is compared to the critical/allowable value of stress and if this critical value is exceeded, delamination failure is initiated (Mouritz et al. 1997b). Researchers (Ye, 1988; Pearce, 2010) have proposed delamination criteria based on the interaction between the normal and through-thickness shear stresses, interlaminar normal and shear components.

The second approach is the fracture mechanics-based approach, initially suggested by Griffith (1921), suggested that a crack would propagate if available energy exceeds the energy required to create the surfaces of the crack. Irwin (1948; 1958) modified this approach and suggested that a critical elastic strain energy release rate (SERR), or crack extension force, GC, describes the fracture toughness. The most widely employed delamination criteria is VCCT, proposed by Rybicky and Kanninen (1977), which is an extension to finite element analysis (FEA) of Irwin's crack-closure integral (Irwin, 1957). VCCT is based on the assumption that the energy released during crack propagation is the same as the energy required closing the crack (Orifici et al., 2007). VCCT is applicable for both shell and solid models based on SERR. The main drawback of VCCT is the requirement for the pre-existence of a crack front. The fracture-mechanics approaches rely on the definition of an initial flaw or crack, however, in a practical situation, the location of damage initiation is not obvious.

Cohesive damage models have been developed based on damage mechanics to simulate the onset and growth of fractures. They do not depend on a predefined defect. The cohesive elements combine the aspects of strength-based analysis to predict the onset of damage at the interface and fracture mechanics to predict the propagation of a delamination. Interface elements are separate finite element entities, which are modelled between the substructures of a composite material as a means of inserting a damageable layer for delamination modelling. Interface elements can be modelled in various ways from nodal two-dimensional (2-D) spring connections (Cui & Wisnom, 1993; Lammerant & Verpoest, 1996) to full 3-D solid element formulations (Goyal et al. 2004; Petrossian & Wisnom, 1998; de Moura et al. 2000).

© 2015, QuEST Global Services

These elements are designed to represent separation at the zero-thickness interface between the layers of 3D elements during delamination. Also the elements are sufficiently stiff in compression to prevent interpenetration of the delaminated surfaces. The main advantage of the use of cohesive elements is its capability to predict both onset and propagation of delamination without previous knowledge of the crack location and propagation direction. However, it is limited to a very fine mesh and can produce unacceptably inaccurate predictions when large elements are employed. According to Turon et al. (2007), cohesive elementsare an efficient approach to model fracture when the crack propagation is known a priori.

In the current study, interface elements are used to simulate the onset and progression of delamination. The constitutive behaviour of these elements is expressed in terms of tractions versus displacements between the top and bottom edge/surface of the elements (Fig. 3).

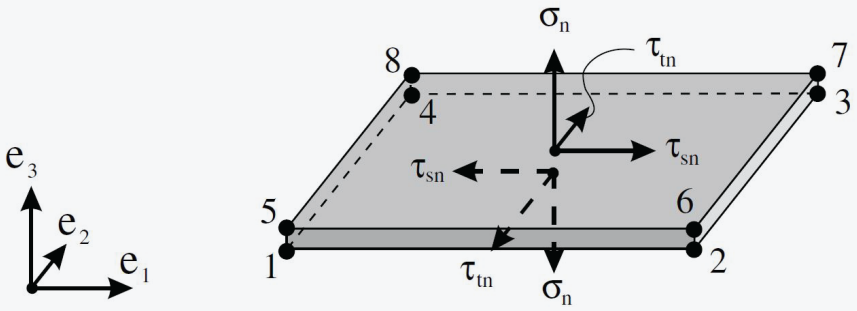

Fig. 3. Three-dimensional stress state of a solid-like interface element (Balzani & Wagner, 2008)

Element 188 in MSC MARC MENTAT 2010 designed for a cohesive zone element, which is a linear, eight-node, 3D element typically used to model the interface between different materials. For a 3D interface element, relative displacement components are given by one normal and two shear components, expressed with respect to the local element co-ordinate system shown in Equation (1).

$$\begin{aligned} \sigma_n &= u_1^{top} - u_1^{bottom} \\ \tau_{sn} &= u_2^{top} - u_2^{bottom} \\ \tau_{tn} &= u_3^{top} - u_3^{bottom} \end{aligned} \qquad (1)$$

Based on relative displacement components, the effective opening displacement is defined as:

$$v = \sqrt{\sigma_n^2 + \tau_{sn}^2 + \tau_{tn}^2} \qquad (2)$$

Damage onset was predicted using a quadratic stress criterion allowing the mesh to split between the materials as shown in Equation (3).

$$\left(\frac{\sigma_n}{S_n}\right)^2 + \left(\frac{\sigma_t}{S_t}\right)^2 = 1 \qquad (3)$$

Where σ_n&σ_t are the normal and tangential stress and S_n,S_t are the critical values of normal and tangential stresses.The tractionseparation model assumes linear elastic behaviour, written in terms of an elastic constitutive tensor K relating the nominal stresses (traction vector) $\tau = (t_n,t_s,t_t)$ to the nominal strains (opening displacement vector) $v(\sigma_n,\tau_{sn},\tau_{tn})$ across the interface. Effective traction is introduced as a function of effective opening displacement and characterised by an initial reversible response, followed by an irreversible response as soon as a critical effective opening displacement has been reached, as shown in Fig. 4.

© 2015, QuEST Global Services

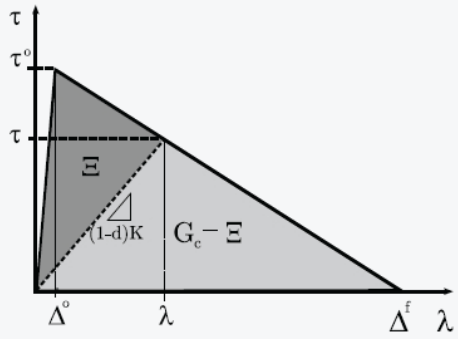

Fig. 4. Damage evolution curve for MSC MARC bilinear cohesive element (34)

The irreversible part is characterised by increasing damage, ranging from zero (onset of delamination) to one (full delamination). The maximum effective traction τ° corresponding to the critical effective opening displacement λ is given by

$$\tau^{o} = \frac{2\,G_c}{\Delta^{f}} \qquad (4)$$

Where Δ^f is the maximum effective opening.

Once the corresponding initiation criterion is reached, the specified damage evolution law describes the rate of material stiffness degradation. A scalar damage variable 'D' ($0 \le D \le 1$) represents overall damage in the material and captures combined effects of all active degradation mechanisms. In the current model, a bilinear model is used to obtain the traction τ. When overall damage variable reaches its limit D_{max}, at all material points, the cohesive element corresponding to complete fracture of the interface between layers can be removed and is considered as delamination propagation.

Numerical Simulation

Finite element simulation of a curved composite panel is carried out using the commercially available finite element package MSC MARC MENTAT 2010. This solver is capable of performing linear and non-linear stress analysis in a static or dynamic framework. In order for it to be employed in this simulation procedure, the solver is equipped with additional isotropic/orthotropic material models for the description of composite materials to perform the nonlinear static analysis of the structural model.

Geometry

A series of top-hat stiffeners were manufactured using the vacuum infusion process (VIP) (or vacuum assisted resin transfer moulding (VARTM) method) for three different layups. The specimens were cured under vacuum bag for 24 hours at room temperature (20°C). Later they were sliced to required dimension, the edges sanded and thoroughly cleaned with acetone. The FE model for top-hat stiffener is created using the geometry shown in Fig. 5. The crown and flange had radii of 19 and 23 mm, respectively, while specimen width was 100 mm. The web has a 3° offset from y-axis. Width of crown and the height of specimen were both 200 mm. The crown is sandwiched between two 10 mm steel backing plates. The experimental test configuration is shown in Fig. 6.

© 2015, QuEST Global Services

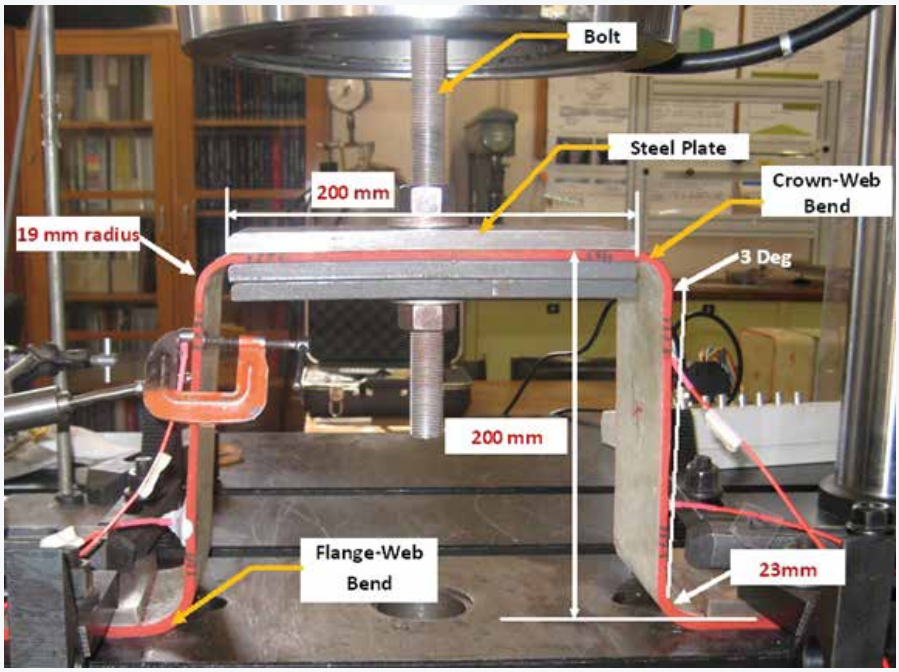

Fig. 5. Top hat stiffener specimen dimensions

Three layups with four fibre types were used: chopped strand mat (CSM), double bias (DB), bi-axial (BE) and unidirectional (UD) fibres. For each layup, flange-web bends had an additional two layers of CSM-450 to stiffen the top-hat stiffener at the base. The three layups of top-hat stiffeners specimens are presented in Table 1.

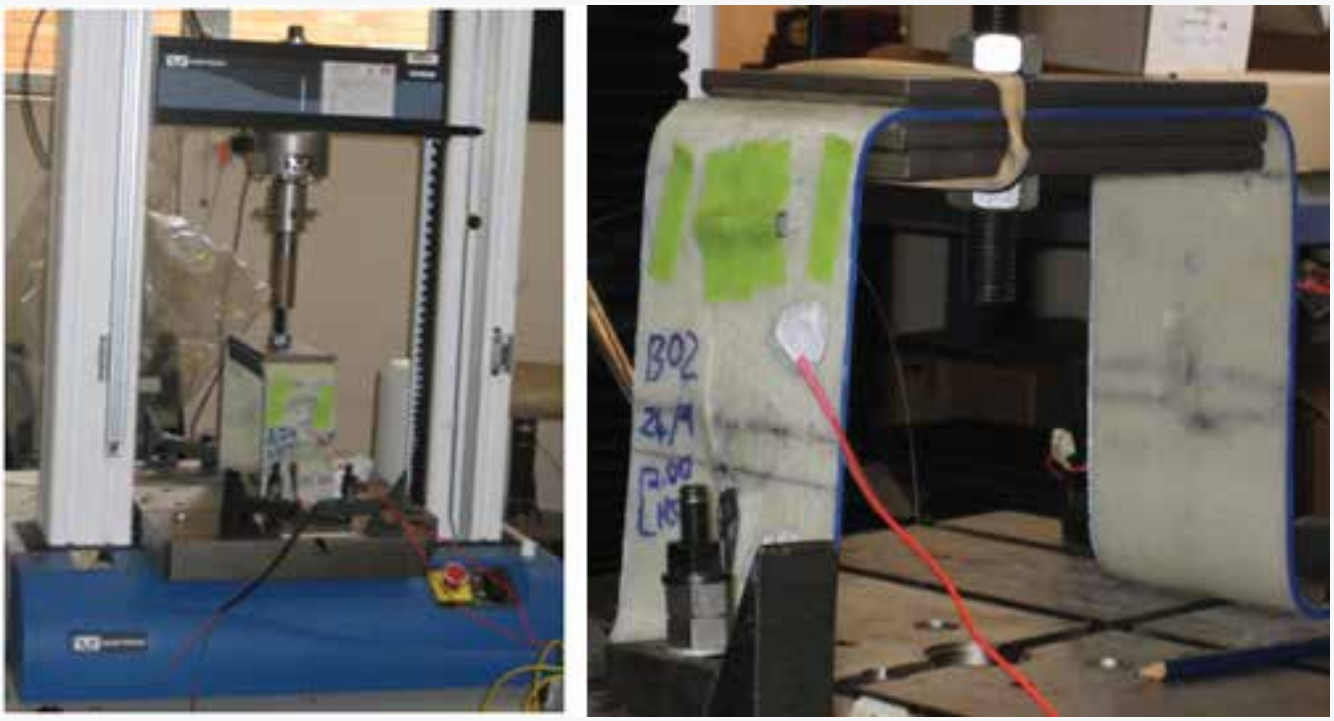

Fig. 6. Experimental test configuration

© 2015, QuEST Global Services

Table 1. VARTM top-hat-stiffener laminate configuration

Layup 1	
CSM+DB	*Thickness*
Mould Surface	*(mm)*
DB-450	0.26
CSM-450	0.6
DB-450	0.26
CSM-450	0.6
DB-450	0.26
CSM-450	0.6
DB-450	0.26
DB-450	0.26
Total thickness	**3.1**

Layup 2	
CSM+DB+UD	*Thickness*
Mould Surface	*(mm)*
CSM-225	0.3
CSM-225	0.3
DB-450	0.26
CSM-225	0.3
DB-450	0.26
CSM-225	0.3
UD-461	0.26
CSM-225	0.3
UD-461	0.26
CSM-225	0.3
Total thickness	**2.84**

Layup 3	
CSM+DB+UD+BE	*Thickness*
Mould Surface	*(mm)*
CSM-225	0.3
DB-450	0.26
CSM-225	0.3
DB-450	0.26
CSM-225	0.3
BE-450	0.465
UD-461	0.26
CSM-225	0.3
BE-450	0.465
UD-461	0.26
Total thickness	**3.17**

Structural Modelling

During experimental investigation, the load was applied at the centre of the crown, using a 20 mm diameter bolt at the centre of the specimen, at a rate of two mm/min (cross-head movement). FEA was performed on a 3D model. Local co-ordinate systems were defined for each element to match the local fibre orientation. Each element thickness represents the thickness of one layer in the composite laminate to obtain an accurate distribution of interlaminar stresses. As observed in the experiments, damage did not occur on both halves of the specimen simultaneously, hence symmetry of the model is not considered. Eight-node isoparametric hexahedral elements (Element type 7, MSC MARC) were used with geometric and material non-linearity. These eight-node composite brick elements allow the definition of layer-by-layer material parameters, layer thickness, and orientation angles for a laminated composite material. Finer mesh with a global edge length of one mm was used around the bend (crown-web interface) to increase the number of elements in the complex geometry. Basic material properties are calculated using 'Component Design Analysis' (CoDA)' software, a standard commercial code for laminate design. The standard material properties are presented in Table 2.

Three boundary conditions were defined to represent the arrangement existing in the top-hat stiffener experimental analysis. Nodes at the flange were secured in all directions and a displacement load was applied on bolt nodes in the y-direction while the steel backing plate nodes were fixed in the z direction. Load was applied linearly with respect to time. Contact condition was modelled using the direct constraint method in MSC MARC. One contact table defined the contact bodies which are likely to be in contact with each other (may be either glued or touching contact) for each increment. Four contact bodies - laminate, upper backing plate (crown top), lower backing plate (crown bottom) and central bolt were defined in the FE model. The nodes of upper and lower backing plates were glued (by defining them in the contact table) to the bolt nodes. The laminate nodes were modelled as touchingthe steel plates.

Table 2. VARTM Top-hat-stiffener laminate configuration

Vacuum Infusion Process Material Properties			
Property	**CSM**	**DB**	**UD**
E11 (MPa)[b]	10000	6703	37232
E22 (MPa)[b]	10000	6703	15128
E33 (MPa)[c]	6500	6173	15128
υ12 (MPa) [c]	0.347	0.62	0.369
υ23 (MPa) [c]	0.139	0.146	0.249
υ31 (MPa) [c]	0.108	0.133	0.087
G12 (MPa)[c]	2602	7157	2265
G23 (MPa)[c]	1847	2050	1847
G31 (MPa)[c]	1847	2050	2265
ILTS (MPa)[a]	9.5	10.5	10.5
ILSS (MPa)[a]	28	30	28
Flexure Modulus (MPa)[b]	2668	2869	6748
Flexure Strength (MPa)[b]	266	177	579
Fracture Toughness G_{IC} (kJ/m^2)[a]	0.68	1.04	0.84
Critical opening displacement (mm)[a]	0.05	0.05	0.05

[a] Literature [Johnson, 1986; Dirand et al., 1996; Perrot et al., 2007; Park and Jang, 2004; Kitching et al., 1984]

[b] Experimental testing

[c] Obtained through 'Component Design and Analysis (CoDA)' software using resin and fibre properties

© 2015, QuEST Global Services

A single load case was defined in the simulation. Generally, a small number of increments provide an inaccurate damage mechanism while a large number of increments increase the computer runtime; hence a reasonable number of increments needs to be provided. After a certain number of iterations, 200 fixed increments (load steps) were given to identify the damage initiation and progression with high accuracy and acceptable processing time.

FEA Results – Layup 1

This layup consists of randomly oriented short-length fibres (CSM) and DB. The numerical analysis was conducted using small strain analysis and steel backing plates were modelled with elastic-plastic behaviour. Interlaminar stress distribution at the upper bend, just before the first failure is shown in Fig. 7.

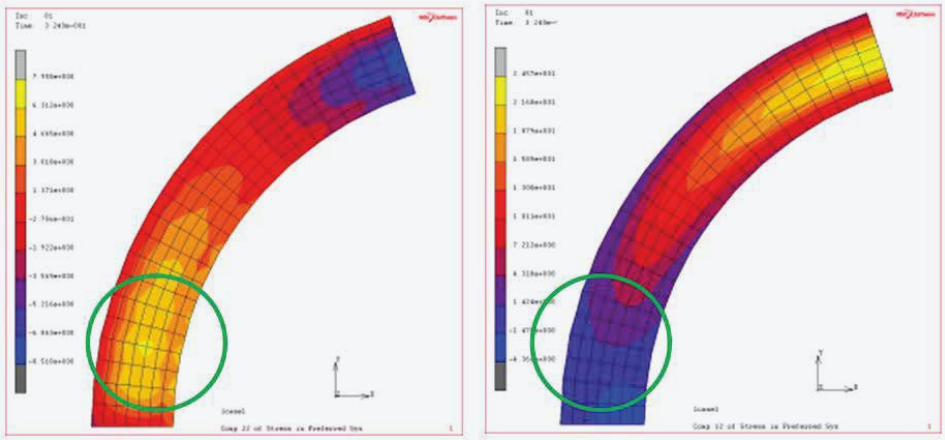

Fig. 7. Layup 1 ILTS (Left) and ILSS (Right) distribution just before first failure

To validate the numerical model, the FEA result was compared with experimental results for specimen 'CSM+DB 02', shown in Fig. 8. When the interlaminar stresses exceed critical values, interlaminar cracks are introduced. Crack growth is obtained by insertion of interface elements.

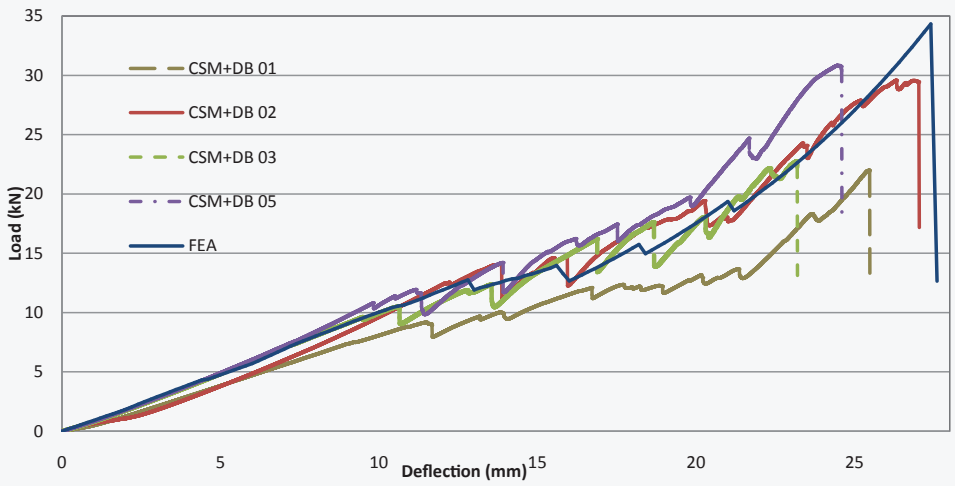

Fig. 8. Layup 1 load-deflection plot — Experiment and FEA comparison

© 2015, QuEST Global Services

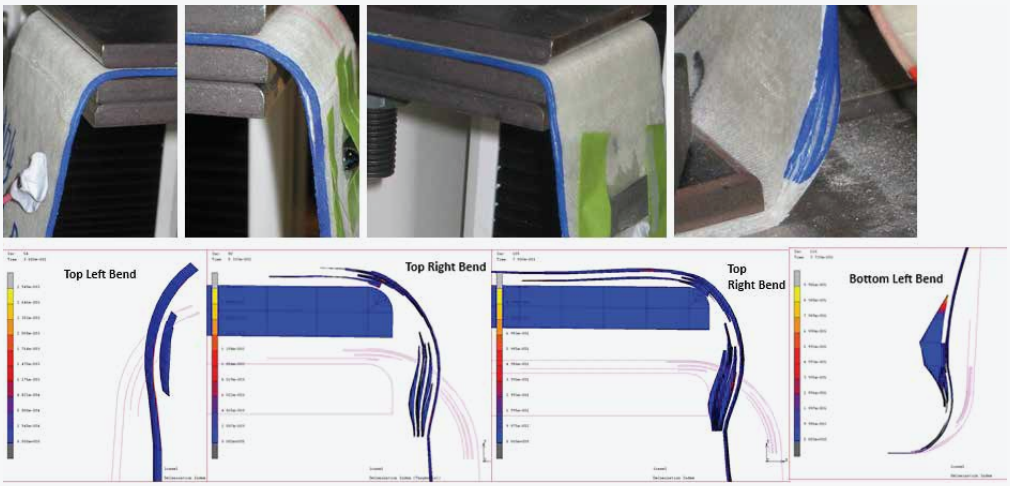

Fig. 9. Layup 1 correlation of Experimental failure and FEA failure prediction

Interlaminar Strain Distribution around bends for VARTM top hat stiffener

The ILTS reached a maximum at the lower end of the left bend and this location was predicted as the probable location of the initial failure. The delamination index just before the first failure is shown in Fig. 10.

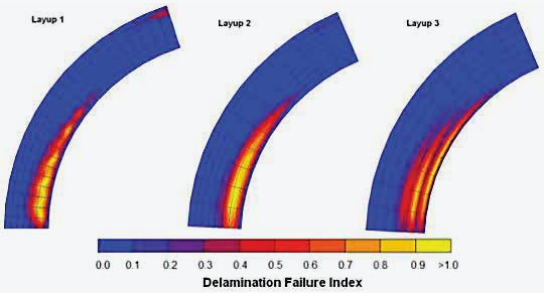

Fig. 10. Delamination failure index at first failure for all three layups at left crown bend

The critical interlaminar tensile and shear stresses of all three layups are shown in Figs. 11 to 16 with the failure locations marked. Figs. 11 and 12 show through-thickness interlaminar tensile and shear stress distributions, whereas Figs. 13 and 14 detail the ILTS and ILSS distributions across the width of the specimen between the second and third layers at an angle of 180 from the bottom of the left-hand bend. Figs. 15 and 16 depict the ILTS and ILSS distributions between the second and third layers around the radius of the bend. As the specimens are symmetric about the vertical axis, stress distribution is the same at both bends until first failure. A ninterlaminar matrix crack occurred due to excessive ILTS and delamination initiated at the lower end of the bend for all three layups.

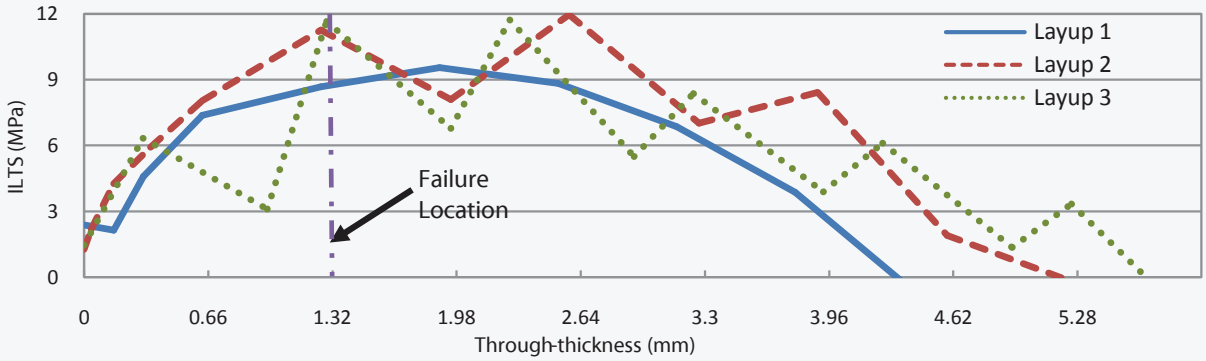

Fig. 11. Through-thickness ILTS distribution

© 2015, QuEST Global Services

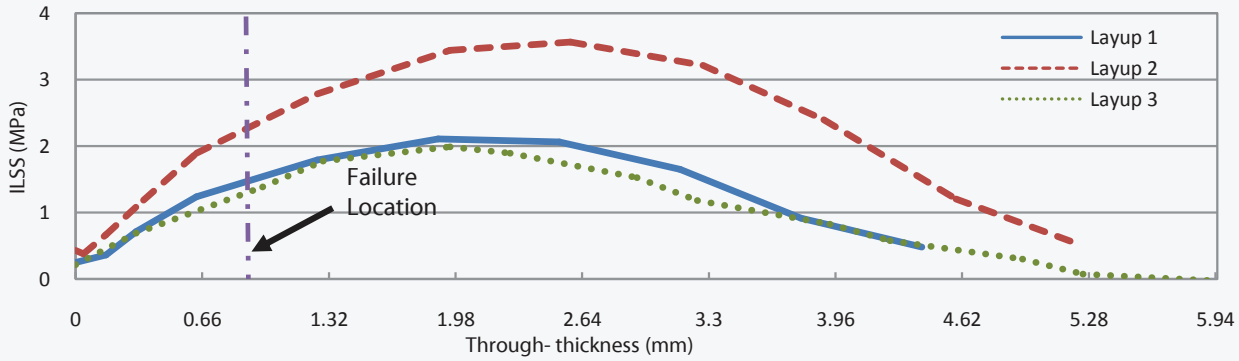

Fig. 12. Through-thickness ILSS distribution

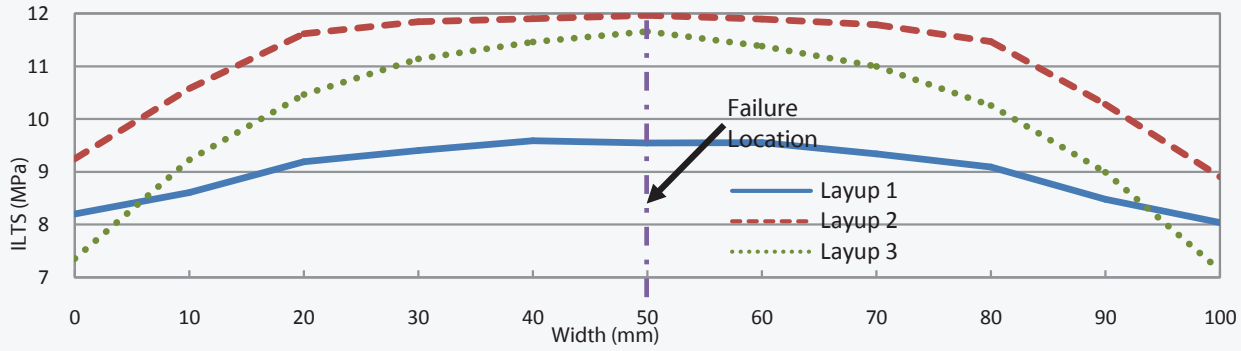

Fig. 13. ILTS distribution across the width

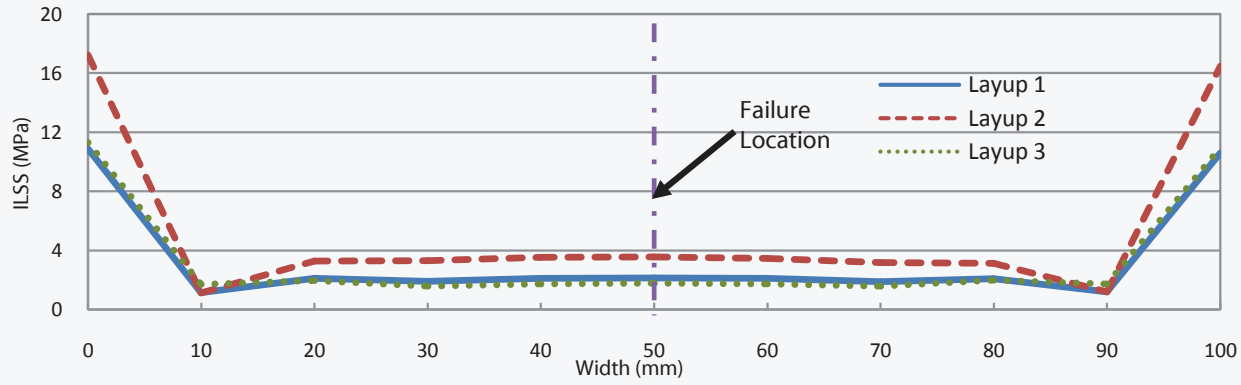

Fig. 14. ILSS distribution across the width

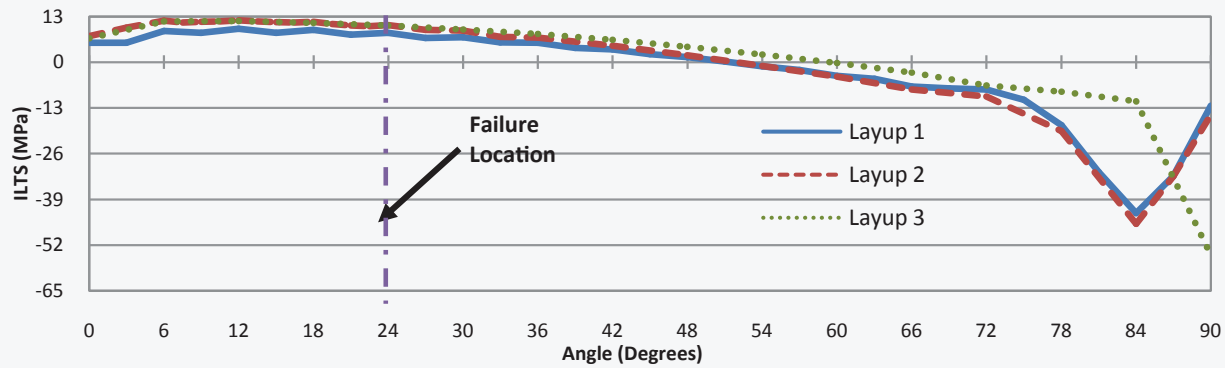

Fig. 15.ILTS distribution along the bend (radius)

© 2015, QuEST Global Services

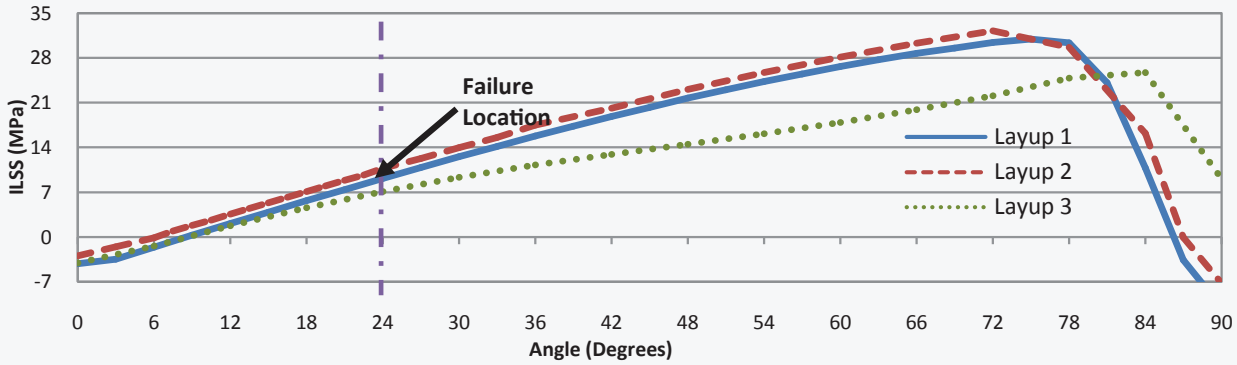

Fig. 16.ILSS distribution along the bend (radius)

Conclusion

In this paper, an experimental and analytical investigation of curved laminates that fail due to delamination is presented. It was observed that a better understanding of the inter-laminar tensile and shear stress distribution makes the design more robust and minimises material and human catastrophy.

FE analysis of GFRP composite top hat stiffeners is presented. Detailed stress distribution around the bends is analysed. Cohesive zone elements are used to simulate the delamination initiation and growth. The contribution of inter-laminar tensile and shear stresses towards failure are investigated. For all three layups, failure initiation occurred between the second and third layers, i.e.180 from the lower end of the bend and along the loading axis of the structure (mid-width of the specimen). From this analysis it was indicated that interface elements can be used to analyse strength and rigidity of the composite structure where delamination is the primary mode of failure.

The top hat stiffener failed at the curved section due to excessive interlaminar stresses. The interlaminar strength is a resin dependent mechanical property in the through-thickness direction. The limiting factor for failure initiation is the opening of the layers (ILTS) rather than sliding of the layers (ILSS). The predictions using FEA are in reasonable agreement with the experiments. Experimental results include scatter and uncertainty whereas the finite element model is free from manufacturing and testing inaccuracies.

Acknowledgements

The authors would like to acknowledge the technical support from EMP Composites, Sydney, Australia for the manufacture of the composite top-hat-stiffener specimens.

References

1) Balzani, C. and Wagner W. An interface element for the simulation of delamination in unidirectional fibre-reinforced composite laminates. Engineering Fracture Mechanics, 2008, 75, 2597-2615.

2) Choi, H.Y., Wu, H.Y., and Chang, F.K. A new approach toward understanding damage mechanisms and mechanics of laminated composites due to low-velocity impact: Part II-Analysis. Journal of Composite Materials, 1991, 25, 1012-1038.

3) Cui, W., and Wisnom, M.R. A combined stress-based and fracture-mechanics-based model for predicting delamination in composites. Composites, 1993, 24(6), 467-474.

© 2015, QuEST Global Services

4) de Moura, M.F.S.F., Goncalves, J.P.M., Marques, A.T., and de Castro P.M.S.T., Prediction of compressive strength of carbon-epoxy laminates containing delamination by using a mixed-mode damage model. Composite Structures, 2000, 50, 151-157.

5) Dirand X., Hilaire B., Soulier J.P. Nardin M. (1996). Interficial shear strength in glass-fiber/vinylester-resin composites. Composites Science and Technology 56, 533-539.

6) Dodkins, A.R., Shenoi, R.A., and Hawkins, G.L. Design of joints and attachments in FRP ship structures, Marine Structures, 1994, 7, 364-398.

7) Eksik, O., Shenoi, R.A., Blake, J.I.R., and Jeong, H.K. Damage mechanisms of hat-shaped GRP beams. Journal of Reinforced Plastics and Composites 2004, 23(14), 1497-1514.

8) Eksik, O., Shenoi, R.A., Moy, S.J., and Jeong, H.K. Finite element analysis of top-hat-stiffened panels of fiber-reinforced-plastic boat structures. Marine Technology 2007, 44(1), 16-26.

9) Goyal, V.K., Jaunky, N.R., Johnson, E.R., and Ambur, D.R. Intralaminar and interlaminar progressive failure analyses of composite panels with circular cut-outs. Composite Structures, 2004, 64(1), 91-105.

10) Graff, E. Mechanical behaviour of thick, curved laminated composites. PhD thesis, Stanford University, 1989.

11) Griffith A.A. The phenomena of rupture and flow in solids. Philosophical Transactions of the Royal Society of London, Series A, 1921, 221, 163-198.

12) Irwin G.R. Analysis of stresses and strains near the end of a crack transversing a plate. Journal of Applied Mechanics, 1957, 24, 361–364.

13) Irwin G.R. Fracture Dynamics. Fracturing of Metals, 1948, 147-166. American Society for Metals symposium (Trans. ASM 40A), Cleveland, USA.

14) Irwin G.R. Fracture. Handbuch der Physik, Flügge, ed., 1958, 558-590.

15) Johnson A.F. (1986). Comparison of the mechanical properties of SMC with laminated GRP materials. Composites 3, 233-239.

16) Junhou, P., and Shenoi, R.A. Examination of key aspects defining the performance characteristics of out-of-plane joints in FRP marine structures. Composites Part A, 1996, 27A, 89-103.

17) Kaczmarek, K., Wisnom, M.R., and Jones, M.I. Edge delamination in curved (0(4)/±45(6)S glass-fibre/epoxy beams loaded in bending. Composite Science and Technology, 1998, 58, 155–161.

18) Kedward, K.T., Wilson, R.S., and McLean, S.K. Flexure of simply curved composite shapes. Composites, 1989, 20(6), 527-536.

19) Kitching R., Tau A.L., Abu-Mansour T.M.N. (1984). The influence of through thickness properties on glass reinforced plastic laminated structures. Composite Structures. 2, 105-151.

20) Lammerant, L., and Verpoest, I. Modelling of the interaction between matrix cracks and delaminations during impact of composite plates. Composites Science and Technology, 1996, 56, 1171-1178.

21) Lekhnitskii, S.G. Anisotropic Plates, Gordon and Breach Science Publishers, New York, 1968. 22) Martin, R,H., and Jackson, W.C. Damage Prediction in Cross-Plied curved composite laminates. Composite Materials, Fatigue and Fracture, 1993, 4, 105-126.

23) Mouritz, A.P., Gallagher, J., and Goodwin, A.A. Flexural strength and interlaminar shear strength of stitched GRP laminates following repeated impact. Composites Science and Technology, 1997b, 87, 509-522.

24) Mouritz, A.P., Leong, K.M., and Herszberg I. A review of the effect of stitching on the in-plane mechanical properties of fibre-reinforced polymer composites. Composites Part A, 1997a, 28, 979-991.

25) Orifici, A.C., Thomson. R.S., Degenhardt. R., Bisagni. C., and Bayandor, J. Development of a finite-element analysis methodology for the propagation of delaminations in composite structures. Mechanics of Composite Materials, 2007, 43(1), 9-28.

26) Park R., Jang J. (2004). Effect of surface treatment on the mechanical properties of glass fiber/vinylester composites. Journal of Applied Polymer Science. 91, 3730-3736.

27) Pearce, G.P. High Strain rate behaviour of bolted joints in carbon fibre composite structures, PhD Thesis, University of New South Wales, Sydney, 2010.

© 2015, QuEST Global Services

28) Perrot Y., Baley C., Grohens Y. and Davies P. (2007). Damage resistance of composites based on glass fibre reinforced low styrene emission resins for marine applications. Applied Composite materials 14, 67-87.

29) Petrossian, Z., and Wisnom, M.R. Prediction of delamination initiation and growth from discontinuous plies using interface elements. Composites Part A – AppliedScience and Manufacturing, 1998, 29(5-6), 503-515.

30) Phillips, H.J., Shenoi, R.A., and Moss, C.E. Damage mechanics of top-hat stiffeners used in FRP ship construction. Marine Structures, 1999, 12, 1-19.

31) Prusty, B.G. Linear static analysis of composite hat-stiffened laminated shells using Finite elements. Finite Elements in Analysis and Design 2003, 39, 1125–1138.

32) Prusty, B.G., Ray, C., and Satsangi, S. Progressive failure analysis of laminated unstiffened and stiffened composite panels. Journal of Reinforced Plastics and Composites, 2005, 24(6), 633-642.

33) Raju, Prusty, B.G., Kelly, D.W., Lyons, D., and Peng, G.D. Top Hat Stiffeners: A Study on Keel Failures. Ocean Engineering 2010, 37(13), 1180-1192.

34) Rybicky, E.F., and Kanninen, M.F. A finite element calculation of stress intensity factors by a modified crack closure integral. Engineering Fracture Mechanics, 1977, 9(4), 931-938.

35) Shenoi, R.A., and Hawkins, G.L. An investigation into the performance characteristics of top-hat stiffener to shell plating joints. Composite Structures.1995, 30, 109-121.

36) Shenoi, R.A., and Wang. W. Through-thickness stresses in curved composite laminates and sandwich beams. Composites Science and Technology, 2001, 61, 1501-1512.

37) Sridharan, S. Delamination behaviour of composites. Boca Raton, FL:CRC Press, 2008.

38) Turon, A., Da´vila, C.G., Camanho, P.P., and Costa J. An engineering solution for mesh size effects in the simulation of delamination using cohesive zone models, Engineering Fracture Mechanics, 2007, 74, 1665–1682.

39) Wisnom, M.R. 3-D Finite element analysis of curved beams in bending. Journal of Composite Material, 1996, 30(11), 1178–1190.

40) Ye, L. Role of matrix resin in delamination onset and growth in composite laminates. Composites Science and Technology, 1988, 33(4), 257-277.

© 2015, QuEST Global Services

Author Profile

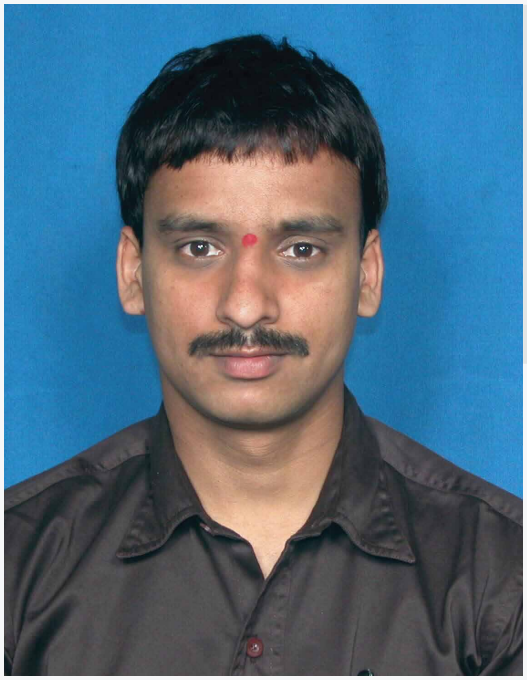

Dr. Raju

MTech and PhD from UNSW, Australia. Over 14 years of experience in Structural analysis of metal and Composite Structures. Working in Airbus ODC and Professor at VTU, Bangalore. Active participation in NASSCOM and SAE initiatives for Industry-Academia interaction. Supporting Board of Studies for Aerospace Engineering, VTU, Karnataka. Has over 50 refereed publications in International Journals, Conferences and Book chapters. Areas of interests are: Damage mechanics; Progressive failure analysis; Structural Health Monitoring; Fatigue and Damage tolerance; Damage prediction and analysis of Metallic and Composite structures. Certified Naturalist and Yoga Teacher.

About QuEST Global

QuEST Global is a focused global engineering solutions provider with a proven track record of over 17 years serving the product development & production engineering needs of high technology companies. A pioneer in global engineering services, QuEST is a trusted, strategic and long term partner for many Fortune 500 companies in the Aero Engines, Aerospace & Defence, Transportation, Oil & Gas, Power, Healthcare and other high tech industries. The company offers mechanical, electrical, electronics, embedded, engineering software, engineering analytics, manufacturing engineering and supply chain transformative solutions across the complete engineering lifecycle.

QuEST partners with customers to continuously create value through customer-centric culture, continuous improvement mind-set, as well as domain specific engineering capability. Through its local-global model, QuEST provides maximum value engineering interactions locally, along with high quality deliveries at optimal cost from global locations. The company comprises of more than 7,000 passionate engineers of nine different nationalities intent on making a positive impact to the business of world class customers, transforming the way they do engineering.

QUEST

BORN TO ENGINEER

http://quest-global.com

© 2015, QuEST Global Services